

Spectroscopic studies involving two-step processes in the reaction $^{28}\text{Si}(d,p)^{29}\text{Si}(\frac{5}{2}^+)$

R. N. Boyd, J. Kaminstein, R. Arking,* and H. Clement†

Nuclear Structure Research Laboratory, ‡ University of Rochester, Rochester, New York 14627

(Received 9 September 1974; revised manuscript received 22 April 1975)

Particle- γ -ray angular correlations have been studied in the $^{28}\text{Si}(d,p)^{29}\text{Si}(\frac{5}{2}^+, 2.03 \text{ MeV})$ reaction and subsequent γ -ray decay to the ^{29}Si ground state. The calculated correlations represent the data well near the stripping peak, and show appreciable sensitivity to the details of the two-step reaction processes. This sensitivity allows the determination of structure information about excited core components of the nuclear wave function.

NUCLEAR REACTIONS $^{28}\text{Si}(d,p\gamma)$, $E=7.6 \text{ MeV}$; proton- γ -ray angular correlations, ^{29}Si deduced effect of inelastic processes on angular correlations; natural target.

I. INTRODUCTION

Recently, the two-step reaction mechanism has been applied to nuclear transfer reaction studies^{1,2} to explain effects which could not be described within the constructs of the simple distorted-wave Born approximation (DWBA). These studies have involved only differential cross section measurements; indeed the existence of an observable cross section was, in many of the cases studied, sufficient to require two-step processes.

Reactions in which both one- and two-step processes are involved present a less definitive situation than that in which the former are clearly inhibited. The $^{28}\text{Si}(d,p)^{29}\text{Si}(\frac{5}{2}^+, 2.03 \text{ MeV})$ reaction is an example of such a situation. Many studies of this reaction have been performed in the past,³⁻⁶ with the generally accepted result being that the spectroscopic factor for this level is about $S=0.12$. Furthermore the usual DWBA seemed adequate for reproduction of the differential cross section around the stripping peak, and uncertainties in the optical model parameters and compound nuclear effects are large enough to explain discrepancies between theory and data at scattering angles away from this peak.

The present study, a preliminary report of which was given earlier,⁷ shows that the agreement which exists between experiment and theory is somewhat fortuitous. In fact calculated differential cross sections assuming (1) one-step transfer, (2) a full treatment of the reaction, involving both one- and two-step processes, and assuming the form of the wave functions for the levels involved which is suggested by theory,⁸ and (3) another full calculation assuming an alternate but reasonable wave function for the $^{29}\text{Si}(\frac{5}{2}^+)$ state, all give essentially the same differential cross

section around the stripping peak.

Thus we have studied proton- γ -ray angular correlations (PGAC) to attempt to achieve sensitivity to the pieces of the wave functions involved in the two-step reaction processes. Our studies show that, even near the stripping peak, such sensitivity does exist, and that the PGAC are sensitive not only to the form and strength of the two-step processes, but to the relative phase between one- and two-step reaction trajectories.

Essential features of the data acquisition system are discussed in Sec. II. Details of the various calculations and comparison to the PGAC data are presented in Sec. III. Section IV then presents the conclusions drawn from our study.

II. EXPERIMENTAL DETAILS

The PGAC were measured using the University of Rochester MP tandem Van de Graaff accelerator in conjunction with the particle- γ -ray correlation setup. In this setup, six NaI(Tl) γ -ray detectors, located 15 cm from the target, can be operated in arbitrary coincidence with four particle detectors. A hemispherical scattering chamber lid and overhead detector mounting bar allows for the γ -ray detectors to be placed both in and out of the reaction plane. The proton detectors were 1500 μm thick surface barrier detectors having 50 mm surface area and were located in the horizontal plane so as to subtend an angle of $\pm 2.5^\circ$. These detectors had 0.1 mm thick Al absorbers in front of them to degrade the deuteron energies with respect to the proton energies, thus allowing for discrimination of the $^{28}\text{Si}(d,p\gamma)$ events taking place in the target from those initiated in the (Si) detectors. The coincidences between particle and γ -ray detectors were determined using

a fast electronics setup, the details of which are given in Ref. 9. Data were recorded event by event on magnetic tape utilizing the University of Rochester PDP 6-PDP 8 on-line computer system and were analyzed off line with the same facility.

The coordinate system defining the location of the γ -ray and particle detectors is as follows. The \hat{z} axis is in the direction of $\vec{k}_{in} \times \vec{k}_{out}$, and thus is normal to the (horizontal) reaction plane.

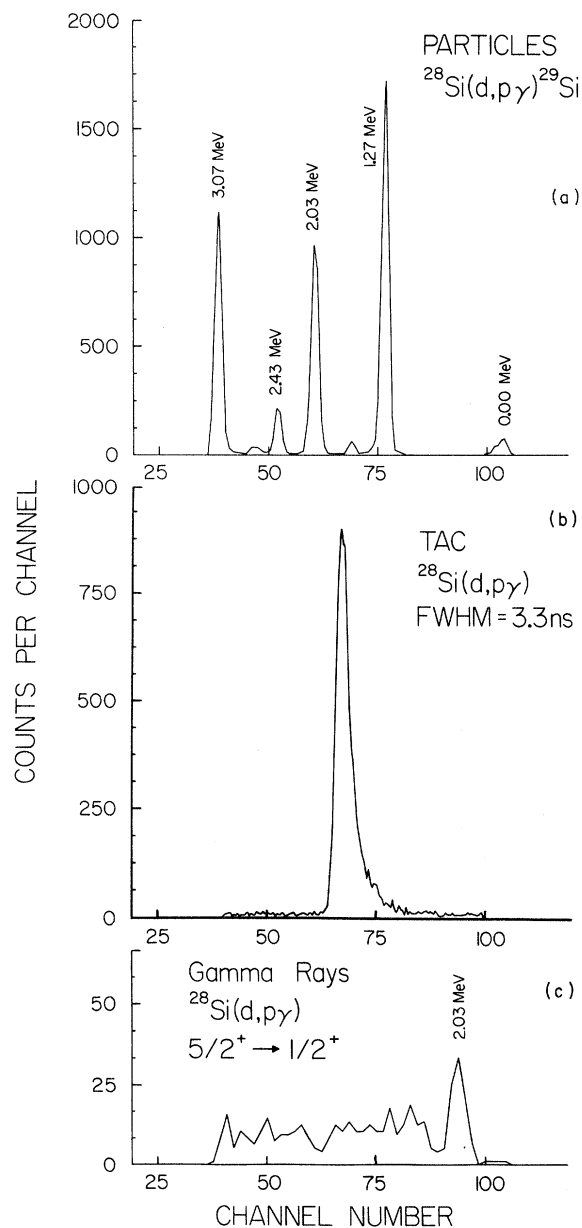


FIG. 1. Typical experimental spectra: (a) the coincident proton spectrum (b) the time-to-amplitude converter spectrum, and (c) the spectrum of γ rays gated with the time peak and 2.03 MeV proton group.

Then θ_γ is the γ -ray polar angle with respect to the vertical direction. The angle ϕ_γ is the γ -ray azimuthal angle, defined to be zero in the incident beam direction. Since the polar angle for the particle detectors was always 90° , the locations of these detectors are characterized only by their azimuthal angle ϕ_p .

Data were taken for two γ -ray detector polar angles, $\theta = 45$ and 90° . About 20 settings of $(\theta_\gamma, \phi_\gamma)$ were taken in coincidence with each particle detector setting, with most of these data points being measured more than once. Reliable data were measured for particle detector center-of-mass angles of $\phi_p = 47$ and 62° , and data were previously

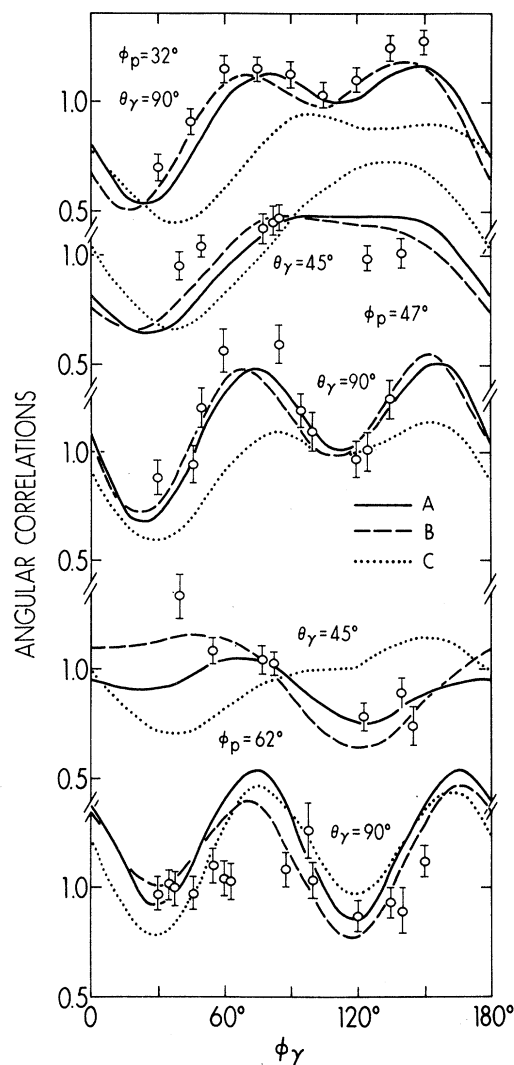


FIG. 2. PGAC data and calculations. Solid curve: calculation A, dashed curve: calculation B, and dotted curve: calculation C. See Sec. III for explanation of each calculation. The $\phi_p = 32^\circ$ data are from Kuehner *et al.* (Ref. 5).

TABLE I. Optical potential parameters:

$$V(r) = V_c(r) + V_R f(x_R) + i4a_I W_D \frac{df(x_I)}{dr} + V_s \chi^2 \frac{1}{r} \frac{df(x_s)}{dr} \bar{\sigma} \cdot \bar{l},$$

where $f(x_j) = [1 + \exp(x_j)]^{-1}$, $x_j = (r - R_j A^{1/3})/a_j$, and

$$V_c(r) \begin{cases} = \frac{Ze^2}{r}, & r > R_c A^{1/3} \\ = \frac{Ze^2}{2R_c A^{1/3}} \left[3 - \frac{r^2}{R_c^2 A^{2/3}} \right], & r \leq R_c A^{1/3} \end{cases}$$

and $\chi^2 = (\text{pion Compton wave length})^2 \approx 2.0 \text{ fm}^2$. Coulomb radius $= 1.32 A^{1/3} = R_c A^{1/3}$. All radii and diffusenesses are given in fm, and all well depths in MeV.

Channel	Real central			Surface imaginary			Spin orbit		
	V_R	R_R	a_R	W_D	R_I	a_I	V_s	R_s	a_s
Elastic deuteron	-101.6	1.25	0.65	16	1.25	0.47	6.5	0.85	0.47
Inelastic deuteron	-102.6	1.25	0.65	16	1.25	0.47	6.5	0.85	0.47
Ground-state proton	-44.0	1.25	0.65	8	1.25	0.47	6.5	0.85	0.47
Excited-state proton	-45.1	1.25	0.65	8	1.25	0.47	6.5	0.85	0.47
Bound-state neutron	a	1.25	0.65				6.5	0.85	0.47

^a Adjusted to give correct binding energies.

measured by Kuehner, Almquist, and Bromley⁵ for a particle detector angle at the stripping peak; about 32°. The latter data were obtained by energy interpolating the data of Ref. 5. The γ rays observed were those from the decay of the $^{29}\text{Si}(\frac{5}{2}^+)$, 2.03 MeV state to the ^{29}Si ground state.

The targets used were 300 $\mu\text{g}/\text{cm}^2$ thick natural Si self-supporting foils. The energy of the incident deuterons was 7.6 MeV. A low incident energy was required to minimize the neutron background. Cross section data used in comparing experiment to theory were determined by energy averaging the results of Kuehner, Almquist, and Bromley⁴ and adjusting the absolute normalization to give an average of the peak values^{2,10} in the literature.

Figure 1 shows typical spectra for the coincident protons [Fig. 1(a)], the time between proton and γ -ray signals [Fig. 1(b)], and the coincident γ rays [Fig. 1(c)], gated with the 2.03 MeV particle group. Since the PGAC data were determined using only the 2.03 MeV γ -ray peak, that spectrum, as shown, is quite adequate for extraction of reliable data. Relative efficiencies of the six γ -ray detectors were checked by redundant measurement of data points with different detectors, and by using other ($d, p\gamma$) reactions in which an excited $J^\pi = \frac{1}{2}^+$ state is observed, the decay from which must be isotropic.

The absolute normalization of the PGAC data was not determined. Thus the set of data points

for each particle detector setting was normalized to give the best fit to the results of calculation D (see Sec. III). The PGAC data are presented in Fig. 2.

III. CALCULATIONS AND COMPARISONS TO DATA

The results of several calculations are presented in this section. The direct-reaction code CHUCK,¹¹ a code which allows a coupled-channel treatment of inelastic scattering as well as two-step calculations, was used to perform these calculations. This code has been modified along the prescription of Rybicki, Tamura, and Satchler¹² to yield the PGAC.

The optical potential parameters used in the calculations were an average of those of Perey¹³ for the proton channels. The Johnson-Soper¹⁴ prescription, using essentially the one-nucleon potentials of Perey,¹³ was used for the deuteron optical potentials. The same geometry was assumed for proton and neutron potentials. The imaginary potentials were reduced from the prescribed¹³ values by 10% to compensate for handling of the inelastic scattering by a coupled-channel procedure. The parameters used in the calculations are listed in Table I. Use of those deuteron parameters gave an appreciably better representation of the PGAC data than did potentials determined from deuteron elastic scattering. The calculated PGAC

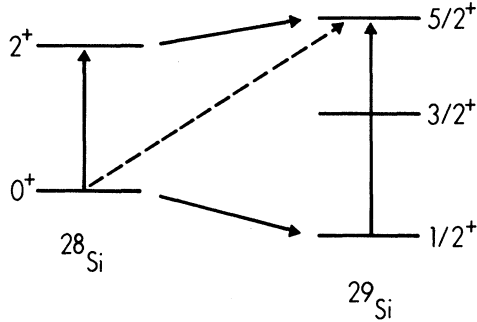


FIG. 3. Reaction trajectories involved in the $^{28}\text{Si}(d, p)^{29}\text{Si}(\frac{5}{2}^+)$ reaction for calculation B.

curves were, in most cases, less sensitive to changes in the optical potentials than were the differential cross sections. The zero-range neutron transfer factor used was $D_0^2 = 1.50$ (Ref. 11).

The full calculations assumed the $^{28}\text{Si}(2_1^+)$ state to be an oblate deformed state, consistent with recent results.¹⁵ Collective form factors (first derivative of real-central and imaginary optical potential terms) were used to characterize inelastic scattering. The magnitude of β_2 , the inelastic scattering scaling parameter, was chosen to be 0.40, a value which is typical¹⁵ of recently published β_2 values.

It was assumed in all the calculations that the reaction was adequately described by local potentials and by the zero-range approximation. In addition, effects of the deuteron D state were neglected. While the effects of these assumptions are not expected to be large, they are currently being investigated.

Within the particle-core coupling formalism, the $^{29}\text{Si}(\frac{5}{2}^+, 2.03 \text{ MeV})$ level is thought⁹ to have a wave function consisting primarily of two pieces, one having a $1d_{5/2}$ neutron coupled to the $^{28}\text{Si}(0^+)$ ground state and the other a $2s_{1/2}$ neutron coupled to the $^{28}\text{Si}(2_1^+)$ first excited state. Thus one could populate the $\frac{5}{2}^+$ state in the $^{28}\text{Si}(d, p)$ reaction via three reaction trajectories, as shown in Fig. 3. In that figure the dashed line indicates the usual one-step transition, going directly from $^{28}\text{Si}(0^+)$ to $^{29}\text{Si}(\frac{5}{2}^+)$ via transfer of a $d_{5/2}$ neutron. Reference 8, however, indicates that only about 12% of the $^{29}\text{Si}(\frac{5}{2}^+)$ wave function has the component $|n_{d_{5/2}} \otimes 0^+\rangle$, and this is verified by the spectroscopic factor for the $^{29}\text{Si}(\frac{5}{2}^+)$ state of 0.12 determined by Mermaz *et al.*³ Reference 8 indicates that almost all of the rest of the wave function is composed of the configuration $|n_{s_{1/2}} \otimes 2_1^+\rangle$. Thus the two-step trajectories shown in Fig. 3 as solid lines, each involving both inelastic scattering and $s_{1/2}$ neutron transfer, are expected to be significant. All three

TABLE II. Wave functions used in the calculations.

Calculation	Wave function coefficient of		
	$ n_{d_{5/2}} \otimes 0^+\rangle$	$ n_{s_{1/2}} \otimes 2_1^+\rangle$	$ n_{d_{3/2}} \otimes 2_1^+\rangle$
A	0.33		
B	0.40	0.92	
C	0.23	-0.97	
D	0.37	+0.80	-0.46
E	0.40		+0.91
F	0.36		-0.93
Ref. 8	-0.3493	+0.9244	+0.0317

of these trajectories were included in the calculations referred to as calculations B and C. The difference between B and C is in the relative phase between the $|n_{d_{5/2}} \otimes 0^+\rangle$ and $|n_{s_{1/2}} \otimes 2_1^+\rangle$ pieces of the wave function: In B the phase is positive and in C negative. Since the rotational cores are assumed to be oblate in both ^{28}Si and ^{29}Si , this means that, near the stripping peak, the one- and two-step reaction trajectories interfere destructively in calculation B and constructively in C. Thus, since the one-step reaction amplitude dominates in this reaction, the coefficient of the $|n_{d_{5/2}} \otimes 0^+\rangle$ configuration (see Table II) will have to be less in C than in B to give the same peak cross section.

The simple shell model predicts that the $d_{5/2}$ orbital is essentially filled at ^{28}Si (this is confirmed by the Ref. 3 result) and that the $s_{1/2}$ and $d_{3/2}$ orbitals are essentially empty. Thus the $^{29}\text{Si}(\frac{5}{2}^+)$ state might also have a significant component consisting of a $d_{3/2}$ neutron coupled to the $^{28}\text{Si}(2_1^+)$ state. This assertion was tested in calculations in which the wave function for this state was assumed to have only $|n_{d_{5/2}} \otimes 0^+\rangle$ and $|n_{d_{3/2}} \otimes 2_1^+\rangle$ components. These calculations are referred to as calculations E and F. In calculation E, the relative phase between the $|n_{d_{5/2}} \otimes 0^+\rangle$ and the $|n_{d_{3/2}} \otimes 2_1^+\rangle$ pieces of the wave function is positive, and in F, negative.

Calculation A is a simple one-step calculation, involving only transfer of a $d_{5/2}$ orbital neutron (represented by the dashed line in Fig. 3). Calculation D involves both one- and two-step transfer, with a mixture of $s_{1/2}$ and $d_{3/2}$ orbital neutrons being involved in the two-step transfer. In calculations A through F the strengths of the transitions from the $^{28}\text{Si}(0^+)$ state to the $^{29}\text{Si}(\frac{1}{2}^+)$ and $^{29}\text{Si}(\frac{3}{2}^+)$ levels were taken from published results.³ The coefficients and phases for the $^{29}\text{Si}(\frac{5}{2}^+)$ level assumed for the various calculations are summarized in Table II.

The results of the calculations are shown in Figs. 2, 4, and 5. Figure 4 illustrates the fact

that calculations D and A (the one-step calculation) give differential cross sections having essentially identical shapes. The solid curve represents A, but D is nearly indistinguishable from it from 20 to 120°. The differential cross sections resulting from calculations B and E were essentially identical with each other near the stripping peak, and are represented by the dashed curve in Fig. 4. The dotted curve represents calculations C and F, which were also very similar in the peak region. The differential cross section data indicated in Fig. 4 were obtained from Ref. 4 as indicated above. It should be noted in comparing cross section data and calculations that compound nuclear processes probably contribute about 0.3 mb/sr, a result which would remove the preference of calculations C or F over the other calculations by the cross section data. Subtraction of a constant 0.3 mb/sr from the differential cross section data leaves these data in reasonable agreement with calculation D, certainly to within the uncertainties produced by optical model parameters. This level of compound nuclear cross section is indicated by the cross section to the ^{29}Si -($\frac{3}{2}^+$, 2.43 MeV) level: it is essentially constant at 0.1 mb/sr at 18 and 13 MeV, and rises to about 0.2 mb/sr at 10.0 MeV². We observed it to be about 0.4 mb/sr at 7.6 MeV. The peak of the cross section to the $\frac{5}{2}^+$ level increases by about the same amount over the same energy range. These observations suggest the compound nuclear contribution of about that amount at the lowest en-

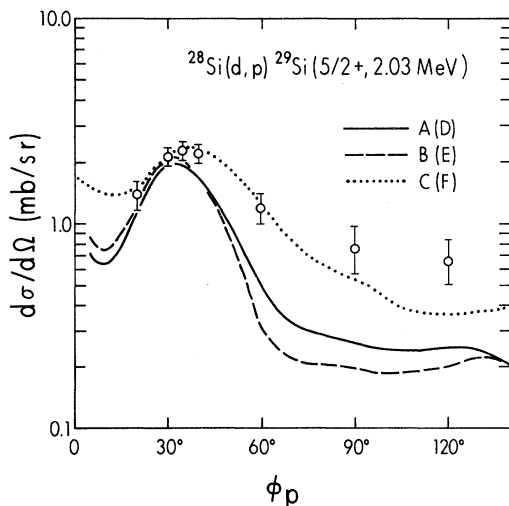


FIG. 4. Differential cross sections. The dots are data points extracted from energy averaging the data of Ref. 4. The bars indicate the fluctuations in this energy region. The solid curve represents calculations A and D, the dashed curve calculations B and E, the dotted curve calculations C and F, as explained in Sec. III.

ergy. Comparison of measured and calculated differential cross sections could be quite misleading at an incident deuteron energy of 7.6 MeV, due to these compound nuclear effects. However, the prominence of the stripping peak above the level of the cross section observed at back angles (about a factor of 6) allows the assumption that the direct reaction mechanism is dominant near the stripping peak. For this reason the PGAC data, shown in Figs. 2 and 5, were all taken with particle detector angles near the stripping peak.

Figure 2 compares the results of calculations A-C with the PGAC data, while Fig. 5 compares

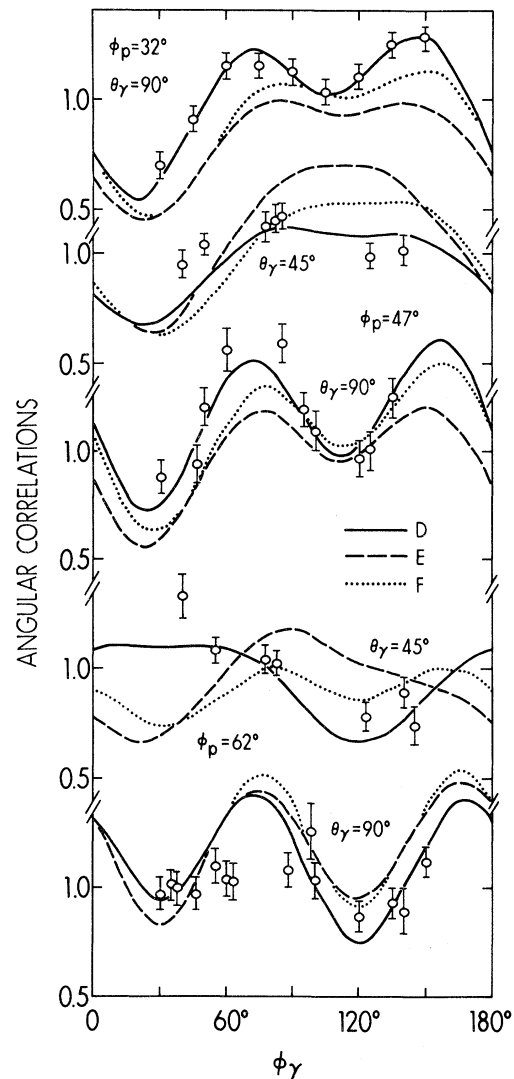


FIG. 5. PGAC data and calculations. Solid curve: calculation D, dashed curve: calculation E, and dotted curve: calculation F. See Sec. III for explanation of each calculation. The $\phi_p = 32^\circ$ data are from Kuehner *et al.* (Ref. 5).

the results of calculations D-F. All of the correlation calculations are compared at particle scattering angles of 32, 47, and 62°. In contrast to the cross section results, the PGAC calculations are strongly dependent on the assumed form of the $^{29}\text{Si}(\frac{5}{2}^+)$ wave function, even when the particle detector is located at the stripping peak. It can also be seen from Figs. 2 and 5 that calculations A, B, and D produce excellent agreement with the data. While calculations A (the one-step result) and B give results similar to that of calculation D, they produce a visibly worse representation of the PGAC data. Furthermore, D produces an acceptable representation of the cross section data, a result not so true of calculation B. Calculation C produces a very different PGAC, and does not even give a qualitative representation of the data. Figure 5 shows that neither of the calculations involving only the $|n_{d_{3/2}} \otimes 2_1^+\rangle$ excited core piece of the wave function can produce a good representation of all of the PGAC data. Thus the PGAC data for the decay of the $^{29}\text{Si}(\frac{5}{2}^+, 2.03 \text{ MeV})$ level exhibit a clear preference for representation of that level by a wave function having a principle excited core piece of $|n_{s_{1/2}} \otimes 2_1^+\rangle$ rather than $|n_{d_{3/2}} \otimes 2_1^+\rangle$. Furthermore, the PGAC require that the phase between the one- and the major two-step reaction trajectories must be such as to give destructive interference at the stripping peak. Finally, although little qualitative difference exists between the PGAC results of calculations D and B, the cross section data are appreciably better represented by the former calculation. This last result suggests that the dominant excited core piece of the wave function for this level does contain the $|n_{s_{1/2}} \otimes 2_1^+\rangle$ component, but that a smaller component of $|n_{d_{3/2}} \otimes 2_1^+\rangle$ must also exist.

IV. CONCLUSIONS

The present study deals with two questions. First of all, is our present characterization of light ion induced reactions capable of reproducing not only differential cross sections, but even such detailed data as the PGAC data presented here? Secondly, do the PGAC show sufficient sensitivity to the two-step processes, at least in cases for which the one-step spectroscopic factor is around 0.1 or less, to draw some conclusions about higher order pieces of the wave functions? Both questions are answered affirmatively.

The spectroscopic factor for the piece of the wave function represented by $|n_{d_{5/2}} \otimes 0^+\rangle$ was predicted to be 0.12 from the work of Castel, Stewart, and Harvey,⁸ while in our analysis the value needed to fit the main stripping peak of the differential cross section data was 0.18. That value also pro-

duced the best fit to the PGAC, although the latter fits are fairly insensitive to changes in the one-step spectroscopic factor of 20% or less. Furthermore the interference between one- and the major two-step trajectories indicated by the Ref. 8 wave functions is destructive, as in our calculations B and D. Thus, even though representation of the differential cross section data required an appreciably larger $|n_{d_{3/2}} \otimes 2_1^+\rangle$ wave function component than indicated by Ref. 8, qualitative agreement does exist between the theoretical wave function and that determined from our study.

The recent study of the $^{28}\text{Si}(d, p)$ reaction by Coker, Udagawa, and Hoffmann² applied calculations similar to the present ones, but examined only cross section data. The wave function used in that study is very much like that used in our calculation C. While that calculation gave a reasonable fit to the 7.6 MeV cross section data, such a calculation completely failed to reproduce even the general features of the present PGAC data. Recently, a study of the $^{28}\text{Si}(\vec{d}, p\gamma)^{29}\text{Si}$ reaction¹⁶ was performed in which PGAC were measured as in the present experiment (but only for $\theta_\gamma = 90^\circ$) but in which the reaction was initiated by a vector polarized deuteron beam. Preliminary comparisons between calculations of the polarized correlations and the data corroborate the present result: The results of calculation D provide an excellent representation of the correlation data, initiated both with polarized and with unpolarized incident deuterons, to the data of the $^{29}\text{Si}(\frac{5}{2}^+)$ level, and an acceptable fit to the cross section data, after compound nuclear contributions were accounted for. Calculations C, E, and F, however, fail to do so. Calculations A and B give a reasonable representation of the data, although they do less well than does calculation D. Thus we feel that the wave function for the $^{29}\text{Si}(\frac{5}{2}^+, 2.03 \text{ MeV})$ level is essentially that used in calculation D.

A possible difficulty in both the present study and that of Ref. 2 is uncertainties in optical model parameters. We have performed calculations similar to the ones presented in this study, but with reduced imaginary strengths in the optical potentials. Those calculations result in appreciably larger cross sections away from the stripping peak, in better agreement with the data. However, the calculated PGAC are very similar to the ones shown here, given the same assumed wave function for the $^{29}\text{Si}(\frac{5}{2}^+)$ level. Thus the optical model uncertainties appear to affect conclusions drawn from comparisons of calculations to cross section data considerably more than those resulting from PGAC information. Because of the uncertainties associated with the cross section data (mostly in the magnitude of the compound nu-

clear contribution) further attempts to improve the fit to those data were not thought to be fruitful.

Further studies under way at both the University of Rochester and at Erlangen,¹⁷ in addition to the work of Ref. 16, should provide further information as to the applicability of PGAC data to nuclear

structure studies.

The authors are grateful to P. D. Kunz for allowing the use of his computer code, and to D. Cline, W. Haeberli, and E. Stephenson for helpful discussions.

*Present address: 2450 East First Street, Brooklyn, New York 11223.

†North Atlantic Treaty Organization Fellow.

‡Supported by a grant from the National Science Foundation.

¹See for example, R. O. Nelson and N. R. Roberson, Phys. Rev. C 6, 2153 (1972); R. J. Ascutto and N. K. Glendenning, *ibid.*, 2, 1260 (1970); A. K. Abdallah, T. Udagawa, and T. Tamura, *ibid.*, 8, 1855 (1973); and references therein.

²W. R. Coker, T. Udagawa, and G. W. Hoffmann, Phys. Rev. C 10, 1792 (1974).

³M. C. Mermaz, C. A. Whitten, Jr., J. W. Champlin, A. J. Howard, and D. A. Bromley, Phys. Rev. C 4, 1778 (1971).

⁴J. Kuehner, E. Almquist, and D. A. Bromley, Nucl. Phys. 21, 555 (1960).

⁵J. A. Kuehner, E. Almquist, and D. A. Bromley, Nucl. Phys. 19, 614 (1960).

⁶H. O. Meyer and J. A. Thompson, Phys. Rev. C 8, 1215 (1973).

⁷R. N. Boyd and J. Kaminsstein, in *Proceedings of the International Conference on Nuclear Structure and*

Spectroscopy, Amsterdam, 1974, edited by H. P. Elok and A. E. L. Dieperink (Scholar's Press, Amsterdam, 1974), p. 178.

⁸B. Castel, K. W. C. Stewart, and M. Harvey, Can. J. Phys. 48, 1490 (1970).

⁹P. M. S. Lesser, Ph.D. thesis, University of Rochester, 1971 (unpublished).

¹⁰D. C. Kocher, P. J. Bjorkholm, and W. Haeberli, Nucl. Phys. A172, 663 (1971).

¹¹P. D. Kunz, University of Colorado, 1973 (unpublished).

¹²F. Rybicki, T. Tamura, and G. R. Satchler, Nucl. Phys. A146, 659 (1970).

¹³F. G. Perey, Phys. Rev. 131, 745 (1963).

¹⁴R. C. Johnson and P. J. R. Soper, Phys. Rev. C 1, 976 (1970).

¹⁵H. Rebel, G. W. Schweimer, J. Specht, G. Schatz, R. Löhken, D. Habs, G. Hauser, and H. Klewe-Nebenius, Phys. Rev. Lett. 26, 1190 (1971).

¹⁶H. Clement, R. N. Boyd, C. Gould, and T. B. Clegg, Bull. Am. Phys. Soc. 20, 573 (1975); private communication.

¹⁷F. Vogler, M. Berg, A. Hofmann, and H. Wagner, Phys. Rev. C 9, 242 (1974).